

Original Research

Metabolism-Related Prognostic Biomarkers, Purine Metabolism and Anti-Tumor Immunity in Colon Adenocarcinoma

Hui Liu^{1,†}, Yuexin Zhang^{2,†}, Quanzheng Zhang³, Tongtong Zhang^{4,5,6,*}, Tianqi Lu^{4,5,6,*}¹Institute of Biomedical Engineering, College of Medicine, Southwest Jiaotong University, 610031 Chengdu, Sichuan, China²Colorectal Cancer Center, Department of General Surgery, West China Tianfu Hospital, Sichuan University, 610041 Chengdu, Sichuan, China³Department of Critical Care Medicine, The Third People's Hospital of Chengdu, Affiliated Hospital of Southwest Jiaotong University, 610031 Chengdu, Sichuan, China⁴The Center of Gastrointestinal and Minimally Invasive Surgery, Department of General Surgery, The Third People's Hospital of Chengdu, The Affiliated Hospital of Southwest Jiaotong University, 610031 Chengdu, Sichuan, China⁵The Center of Obesity and Metabolism disease, Department of General surgery, The Third People's Hospital of Chengdu, Affiliated Hospital of Southwest Jiaotong University, 610031 Chengdu, Sichuan, China⁶Medical Research Center, The Third People's Hospital of Chengdu, Affiliated Hospital of Southwest Jiaotong University, 610031 Chengdu, Sichuan, China*Correspondence: 163zttong@163.com (Tongtong Zhang); ticky_lu@126.com (Tianqi Lu)

†These authors contributed equally.

Academic Editors: Sung Eun Kim and Graham Pawelec

Submitted: 28 April 2023 Revised: 18 July 2023 Accepted: 16 August 2023 Published: 1 December 2023

Abstract

Background: Metabolic reprogramming provides a new perspective for understanding cancer. The targeting of dysregulated metabolic pathways may help to reprogram the immune status of the tumor microenvironment (TME), thereby increasing the effectiveness of immune checkpoint therapy. Colorectal cancer (CRC), especially colon adenocarcinoma (COAD), is associated with poor patient survival. The aim of the present study was to identify novel pathways involved in the development and prognosis of COAD, and to explore whether these pathways could be used as targets to improve the efficacy of immunotherapy. **Methods:** Metabolism-related differentially expressed genes (MRDEGs) between tumor and normal tissues were identified using The Cancer Genome Atlas (TCGA) dataset, together with metabolism-related prognostic genes (MRPGs). Kyoto Encyclopedia of Genes and Genomes (KEGG) pathway enrichment analysis was performed separately for the MRDEGs and MRPGs. Gene Set Variation Analysis (GSVA) was also performed to explore the role of purine metabolism in COAD tumorigenesis. Consensus clustering of purine metabolism genes with the overall survival (OS) of patients and with anti-tumor immunity was also performed. Pearson correlation analysis was used to identify potential targets that correlated strongly with the expression of immune checkpoints. **Results:** A 6-gene signature that had independent prognostic significance for COAD was identified, together with a predictive model for risk stratification and prognosis. The most significantly enriched pathway amongst MRDEGs and MRPGs was purine metabolism. Differentially expressed purine metabolism genes could divide patients into two clusters with distinct prognosis and anti-tumor immunity. Further analysis suggested that purine metabolism was involved in anti-tumor immunity. **Conclusions:** This study confirmed the importance of metabolism-related pathways and in particular purine metabolism in the tumorigenesis, prognosis and anti-tumor immunity of COAD. We identified a 6-gene prognostic signature comprised of *EPHX2*, *GPX3*, *PTGDS*, *NAT2*, *ACO1* and *CPT2*. In addition, four potential immune-metabolic checkpoints (*GUCY1A1*, *GUCY1B1*, *PDE1A* and *PDE5A*) were identified, which could be used to improve the efficacy of immunotherapy in COAD.

Keywords: colon adenocarcinoma; metabolic reprogramming; purine metabolism; immune-metabolic checkpoints

1. Introduction

Colon cancer has the third highest incidence of all malignant tumors, with approximately one million new cases diagnosed worldwide in 2018 and 551,269 patients dying from this disease [1]. Colon adenocarcinoma (COAD) is the most common type of colon cancer. A better understanding of the mechanism of COAD malignancies is urgently needed to help improve therapy.

Metabolic reprogramming is a critical hallmark of human cancer and is an adaptive response to the hypoxic and hypo-nutrient conditions of the tumor microenvironment (TME) [2,3]. Several reprogrammed metabolic pathways

in cancer cells have attracted considerable attention. In particular, enhanced aerobic glycolysis, also known as the Warburg effect, is a well-known alternative metabolic pathway in tumor cells [4]. The Kyoto Encyclopedia of Genes and Genomes (KEGG) database contains approximately 50 metabolism pathways. However, few comprehensive analyses have been conducted to identify the metabolic pathways involved in the poor prognosis of COAD.

There are several ways in which metabolic reprogramming may contribute to the tumor development and progression, including tumor immunity [5–8]. Tumor cells adjust their metabolism to maintain continuous proliferation. Tu-



mor tissue is therefore very different from normal tissue in terms of nutrient intake and waste accumulation. This can impact the presentation and recognition of antigens and impose metabolic stress on infiltrating immune cells, resulting in immune escape [9–12]. Cancer immunotherapy is a major breakthrough in tumor treatment. However, many patients show no response to such therapy, possibly due to abnormal metabolic reprogramming of the immunosuppressive TME, resulting in the regression of the antitumor immune response [13]. Therefore, the targeting of dysregulated metabolism pathways that affect anti-tumor immunity may help to reprogram the immune status of the TME, thereby increasing the effectiveness of immune checkpoint therapy.

The aim of the present study was to identify potential pathways involved in the development and prognosis of COAD, and to explore whether these can be targeted to improve the efficacy of immunotherapy.

2. Material and Methods

2.1 Preprocessing of Transcriptome and Clinical Data

mRNA expression profiles and corresponding clinical information from The Cancer Genome Atlas (TCGA) (<https://portal.gdc.cancer.gov/>) COAD dataset were used as the discovery cohort in this study. Eligible samples met the following criteria: (1) histologically confirmed COAD; (2) mRNA expression profile data and clinical information were both available; and (3) only samples with a patient survival time >30 days were included in the survival analysis. Adjacent normal tissues (n = 40) and COAD samples (n = 404) were used to identify DEGs. The FPKM expression of each gene was applied with Log (1+FPKM) and normalized with Z-score (mean-centered). For external validation, gene expression matrices for the GSE91061, GSE78220, GSE74602, GSE17536, and GSE17537 series were obtained from the Gene Expression Omnibus (GEO) database (<https://www.ncbi.nlm.nih.gov/geo/>). GSE91061 and GSE78220 datasets have high-throughput RNA sequencing information. GSE91061 contains 109 RNA-seq samples (58 on-treatment and 51 pre-treatment) from 65 patients, while GSE74602 contains 30 matched pairs of normal and colorectal tumor samples. GSE78220 contains the RNA-seq transcriptome of responsive (n = 15) and non-responsive (n = 13) pretreated tumors with high-quality RNA (27 pretreatment and 1 early treatment). GSE17536 and GSE17537 contain microarray data from 177 and 55 colorectal cancer patient samples, respectively. The R package “sva” was used to eliminate batch effects that can occur because of the different data sources. To explore the metabolic landscape in colon cancer more comprehensively, genes from all metabolic KEGG pathways were extracted from the Molecular Signature Database (MsigDb) v7.1 (<https://www.gsea-msigdb.org/gsea/msigdb/human/genesets.jsp?collection=CP:KEGG>). A total of 38 metabolic pathways were analysed, includ-

ing alanine aspartate and glutamate metabolism, alpha linolenic acid metabolism, amino sugar and nucleotide sugar metabolism, arachidonic acid metabolism, arginine and proline metabolism, ascorbate and aldarate metabolism, beta alanine metabolism, butanoate metabolism, cysteine and methionine metabolism. The 38 metabolic pathways and the genes within them are listed in **Supplementary Table 1**.

This study was approved by the Institutional Ethics Review Board of the Third People’s Hospital of Chengdu and conducted following the Chinese ethical guidelines for human genome/gene research.

2.2 Bioinformatics Analysis

The R package “limma” was used to perform differentiation analysis of metabolism-related gene expression by comparing tumor and normal samples. The thresholds for DEGs were $|\log_{2}FC| \geq 1$ and adjusted $p < 0.05$. Heatmaps were drawn using the “pheatmap” package and used to visualize differential gene expression.

Univariate analysis and least absolute shrinkage and selector operation (LASSO) Cox regression analysis were performed using the R packages “glmnet” and “survival”. These were used to identify metabolism-related prognostic gene signatures and included only those genes with $p < 0.01$. The risk score for each patient in the training and validation cohorts was calculated separately according to the following formula:

$$\text{Risk score} = \sum \text{coefficient} (mRNA_i) \times \text{expression value}(mRNA_i)$$

The median value of the risk scores was set as the cutoff point, and subsequently used to divide patients into high- and low-risk groups. Survival analysis was performed using Kaplan-Meier (K-M) survival curves. Discrimination between the outcomes for observations and predictions were performed using the area under the curve (AUC) of ROC in the package “survivalROC”. The AUC value ranged 0.5 to 1.0, with 0.5 indicating a random probability and 1.0 indicating perfect predictive ability.

KEGG analysis (p -value ≤ 0.01) was performed using the KEGG automatic annotation web service (<https://www.genome.jp/tools/kaas/>). GSVA was performed using the R package “GSVA” [14]. All genes in the purine metabolism pathway were extracted from the KEGG database using the R package “KEGGREST” (version 1.35.0). Consensus clustering was performed using the R package “ConsensusClusterPlus”. Patients were divided into two clusters according to the expression of DEGs in the purine metabolism pathway. CIBERSORT was performed using the webserver tool (<https://cibersort.stanford.edu/>). Gene Set Enrichment Analysis (GSEA) was performed using GSEA software (<http://www.broadinstitute.org/gsea>). The Gene Expression Profiling Interactive Analysis (GEPIA) database (<http://gepia.cancer-pku.cn/detail.php>) was used to assess the expression level of genes highly related to immune checkpoints. Images of immunohisto-

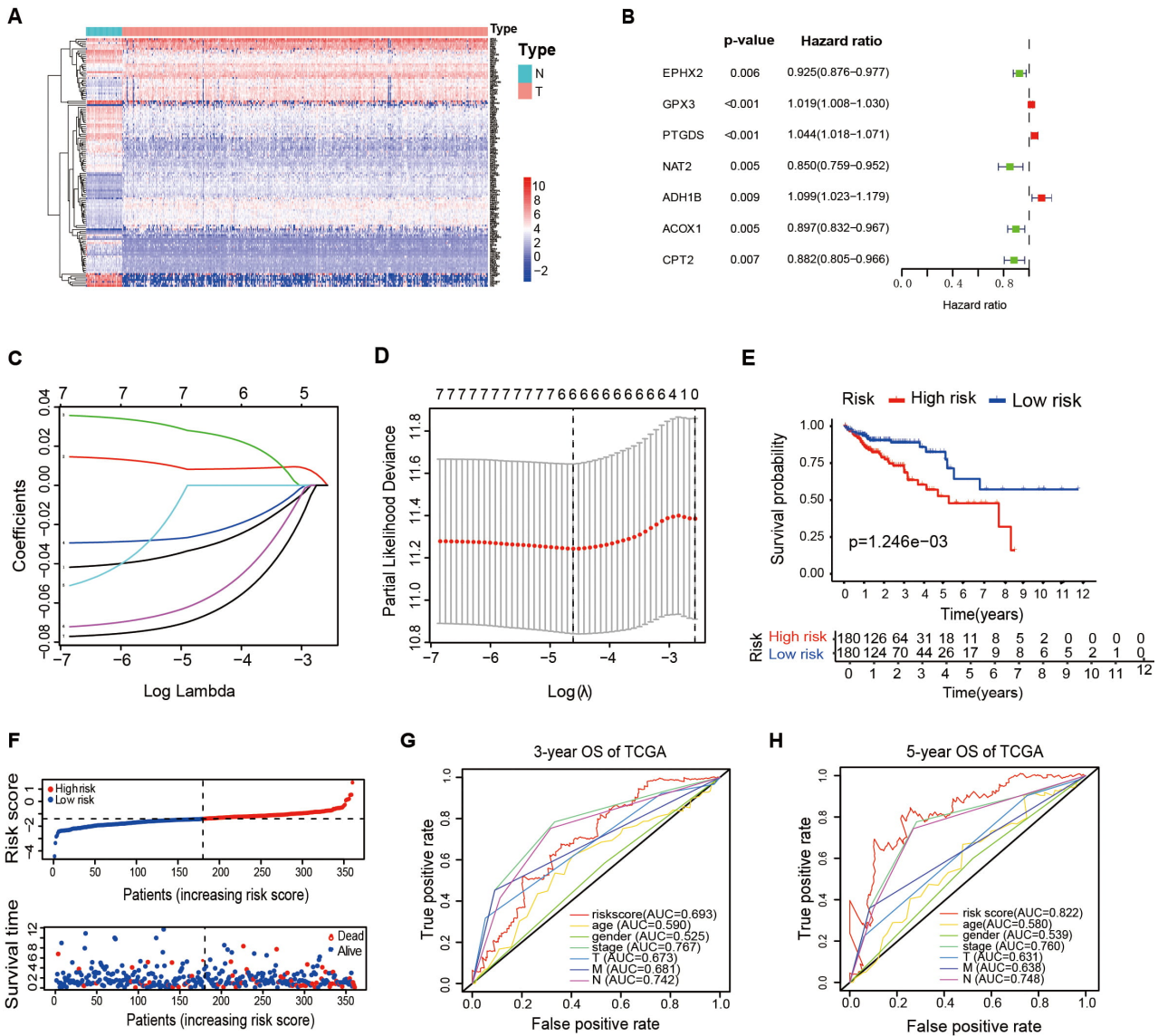


Fig. 1. Construction of a metabolism-related prognostic signature for COAD. (A) Heatmap showing the expression of MRDEGs. (B) Forest plots of univariate analysis for OS in patients from the TCGA database. (C) LASSO coefficient profile for the common genes. (D) Cross-validation for turning parameter screening in the LASSO regression model. (E) Kaplan-Meier survival curves for patients from the TCGA dataset stratified according to their risk score. (F) Distribution of the risk scores and survival times for TCGA patients. (G,H) Receiver operating characteristic (ROC) curve analyses for the prediction of 3- and 5-year OS according to the risk score and other clinical features. COAD, colon adenocarcinoma; MRDEGs, metabolism-related differentially expressed genes; TCGA, The Cancer Genome Atlas; LASSO, least absolute shrinkage and selector operation; OS, overall survival.

chemical staining for the selected core genes in normal tissue and COAD tissue were obtained from the Human Protein Atlas (HPA) database (<https://www.proteinatlas.org/>) [15].

2.3 Immunohistochemistry (IHC) Analysis

Tissues were fixed in 4% PFA at room temperature, embedded in paraffin and sectioned at 3 μ m, then incubated with H₂O₂ to block endogenous peroxidases. Primary antibodies used for IHC analysis included rabbit anti-PDE1A (Proteintech, 12442-2-AP, Wuhan, China), rab-

bit anti-PDE5A (Proteintech, 22624-1-AP, Wuhan, China), rabbit anti-GUCY1A1 (Proteintech, 12605-1-AP, Wuhan, China), and rabbit anti-GUCY1B1 (Proteintech, 19011-1-AP, Wuhan, China). The IHC images were captured using an OLYMPUS v200 ASW microscope. All human participant experiments were conducted in compliance with the ethical standards of the Declaration of Helsinki. This study was approved by the Institutional Ethics Review Board of the Third People's Hospital of Chengdu and conducted following the Chinese ethical guidelines for human genome/gene research.

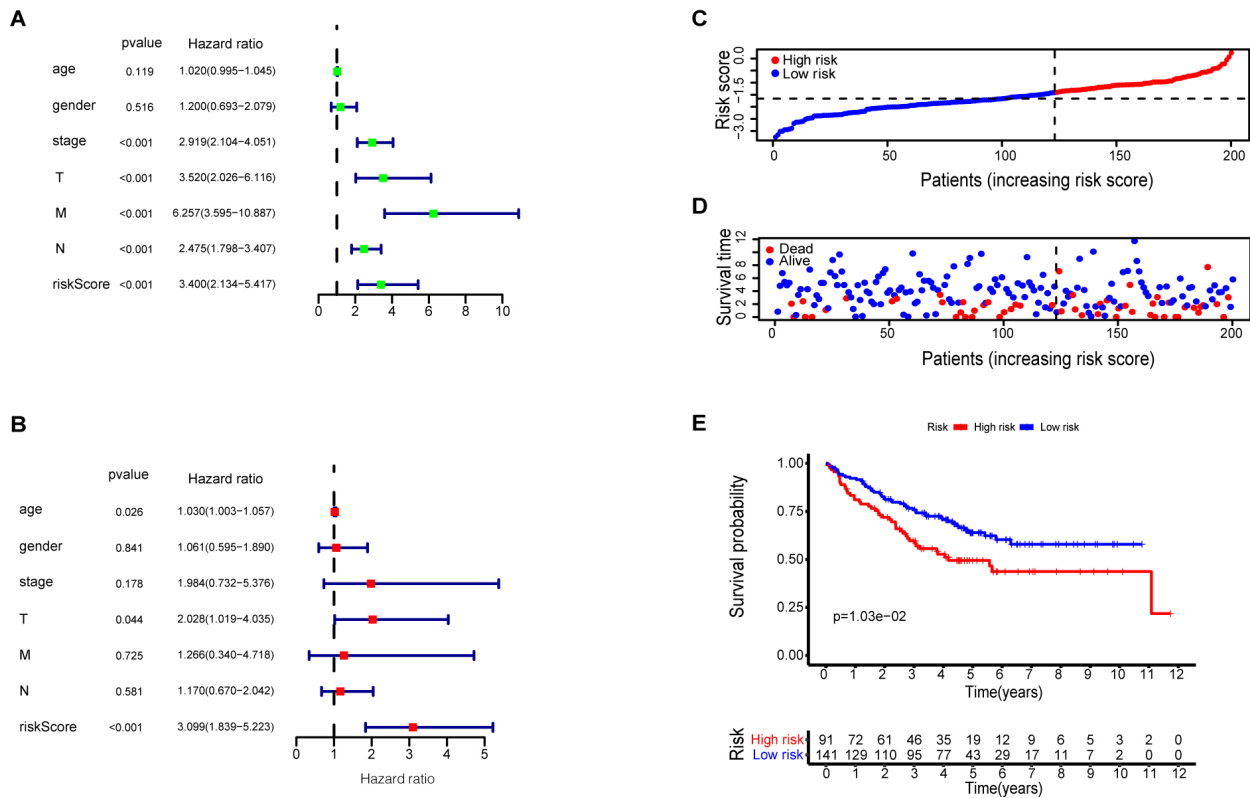


Fig. 2. Validation of the prognostic value of the MRDEG signature. (A) Univariate analysis for the OS of patients from the TCGA database. (B) Multivariate analysis for the OS of patients from the TCGA database. (C,D) Distribution of risk scores and survival times for GEO patients stratified according to their risk score. (E) K-M survival curves for patients in the GEO dataset stratified according to their risk score. GEO, Gene Expression Omnibus; K-M survival curves, Kaplan-Meier survival curves.

2.4 Statistical Analysis

The software package R 3.6.0 (R Foundation for Statistical Computing, Vienna, Austria) was used for statistical analyses. Groupwise comparisons were performed by Wilcoxon-ranked sum testing. Pearson correlation analysis was performed to identify metabolism-related prognostic genes (MRPGs) and potential immune-metabolic checkpoints. The overall survival (OS) rate of patients was estimated using K-M analysis, and the log-rank test was used to evaluate differences between groups. $p < 0.05$ indicated statistical significance.

3. Results

3.1 Identification of a Metabolism-Related Prognostic Signature for COAD

Data for 945 metabolism-related genes was extracted from the KEGG dataset for the differential expression analysis. Using the criteria of adjusted $p < 0.05$ and $|\log_2FC| \geq 1$, a total of 129 MRDEGs were identified (Fig. 1A). Univariate Cox regression analysis was performed to identify MRDEGs with prognostic value, which identified 7 genes with $p < 0.01$ (Fig. 1B). The Lasso regression algorithm with non-zero regression coefficients was used to select the most valuable prognostic genes. Using lasso regres-

sion analysis ($\lambda = 6$), a prognostic model comprised of 6 MRDEGs was constructed (*EPHX2*, *GPX3*, *PTGDS*, *NAT2*, *ACOX1*, and *CPT2*) (Fig. 1C,D). To further validate the prognostic value of this 6-gene signature in COAD, the risk score for each patient in the TCGA and GEO databases was calculated using the formula: $(\text{exprGPX3} \times 0.0083) + (\text{exprPTGDS} \times 0.0269) - (\text{exprEPHX2} \times 0.0314) - (\text{exprNAT2} \times 0.0249) - (\text{exprACOX1} \times 0.0584) - (\text{exprCPT2} \times 0.067)$. All patients were then divided into high- or low-risk groups according to the median risk score (Fig. 1E). The log-rank test found that patients in the high-risk group of the TCGA cohort had significantly shorter overall survival (OS) ($p = 0.0012$; Fig. 1F). The AUCs for 3- and 5-year OS were 0.693 and 0.822 respectively (Fig. 1G,H), and the predictive ability of the signature was better than that of TNM stage.

3.2 Validation of the Prognostic Value of the Metabolism-Related Gene Expression Signature

To determine whether the 6-gene signature was an independent prognostic factor for COAD patients, the expression of these genes was determined using publicly available transcriptome data (TCGA). The expression of *EPHX2*, *GPX3*, *NAT2*, *PTGDS*, *ACOX1*, and *CPT2* were lower in COAD tumor tissue than in normal tis-

sues (**Supplementary Fig. 1A–F**). K-M survival analysis showed that three genes were positively correlated with the OS of COAD patients (**Supplementary Fig. 1G–I**). Patients with high *CPT2*, *EPHX2* and *NAT2* expression levels showed better OS. Additional independent cancer datasets on immunotherapy for melanoma (GSE91061, GSE78220) were used to evaluate the predictive value of these genes for sensitivity to immunotherapy. Patients with higher expression of *PTGDS* were more sensitive to immunotherapy (**Supplementary Fig. 1J**). Patients with high *CPT2* and *NAT2* expression also showed significantly better response to immunotherapy than those with low expression (**Supplementary Fig. 1J**). The above results suggest that patients with high expression levels of *PTGDS*, *CPT2* and *NAT2* are more likely to benefit from immunotherapy.

We next performed univariate and multivariate Cox regression analysis. TNM stage and the risk score showed significant prognostic value for OS in univariate analysis (Fig. 2A). Significant factors were then entered into a multivariate Cox regression model. The 6-gene signature risk score and patient age were found to be independent predictors of OS (Fig. 2B).

To validate the prognostic value of the signature, patients in the GSE17536 and GSE17537 series were separated into high- and low-risk groups according to the 6-gene signature risk score (Fig. 2C,D). Patients in the high-risk group had worse OS than those in the low-risk group (Fig. 2E), thus confirming the prognostic value of the 6-gene signature based MRDEGs.

3.3 Purine Metabolism is the Most Significantly Altered Pathway in COAD and Plays an Important Role in Tumor Development

We next investigated the metabolic pathways involved in determining the prognosis of COAD. KEGG enrichment analysis was performed on the 129 MRDEGs to identify reprogrammed metabolic pathways in COAD. Purine metabolism was found to be the most significantly enriched pathway (Fig. 3A). Other significantly altered pathways were drug metabolism, retinol metabolism, tyrosine metabolism, and pentose and glucuronate interconversion. Pearson correlation analysis was used to identify genes that were co-expressed with the 6-gene signature, using $p < 0.01$ and $|R| > 0.5$ as the cut-off criterion. A total of 615 genes were retained and these were defined as metabolism-related prognostic genes (MRPGs). KEGG enrichment analysis was performed on the MRPGs to identify metabolic pathways that could play a role in determining the prognosis of COAD (Fig. 3B). The results showed that purine metabolism, biosynthesis of antibiotics, pyrimidine metabolism, carbon metabolism, fatty acid degradation, and pyruvate metabolism were associated with the prognosis of COAD patients. Interestingly, and consistent with the results shown in Fig. 3A, the purine metabolism pathway was the most enriched for metabolism-related dif-

ferentially expressed genes ($p = 3.20 \times 10^{-32}$) and also contained the most metabolism-related prognostic genes ($p = 3.14 \times 10^{-74}$). Therefore, its significance in COAD cannot be ignored.

GSVA was used to confirm that purine metabolism played an important role in COAD and to further examine the biological role of purine metabolism in COAD. The GSVA enrichment score was calculated for each patient, who were then divided into two groups according to the median score. The heatmap for the two groups showed a significant difference in the expression of genes for purine metabolism (Fig. 3C). The Wilcoxon test was performed to compare the GSVA enrichment score between patients with different clinical characteristics (Fig. 3D–G). A lower purine metabolism enrichment score was associated with higher tumor-node-metastasis (TNM) stage ($p < 0.05$). Pearson correlation analysis was performed to explore the relationships between purine metabolism and other pathways in the KEGG and hallmark gene sets. The P53 signaling pathway, cell cycle, PI3K/AKT/mTOR signaling, and *MYC* targets were found to be positively correlated with purine metabolism, indicating these pathways were activated (Fig. 3H–K). The above results indicate that purine metabolism plays an essential role in COAD development.

3.4 Consensus Clustering of Purine Metabolism Genes with COAD Patient Survival

In view of the importance of purine metabolism in COAD, we next performed consensus clustering. The $k = 2$ was identified by optimal clustering stability from $k = 2$ to 10 based on the similarity displayed by the expression levels of the MRDEGs and the proportion of ambiguous clustering measure. Patients were divided into cluster-1 ($n = 177$) and cluster-2 ($n = 139$) (Fig. 4A–C). The OS of cluster-1 patients was significantly better ($p < 0.01$) than that of cluster-2 patients (Fig. 4D). The cluster subtypes defined by differentially expressed purine metabolism genes were closely related to the survival of COAD patients, thus further confirming our hypothesis on the important role of this pathway in COAD.

3.5 Consensus Clustering for Purine Metabolism Genes with Anti-Tumor Immunity

GSEA analysis was performed to compare the biological features between the two subtypes. Samples in cluster-2 were more enriched in immune-related pathways, including the immune network for IgA production, natural killer cell-mediated cytotoxicity, antigen processing and presentation, graft versus host disease, and cytokine-receptor interaction (Fig. 5A). These results suggest that purine metabolism may have some interaction with tumor immunity.

The expression of immune checkpoints are closely related to the efficacy of immunotherapy. For example, the overexpression of *PD-L1* is widely used as a predictive biomarker for the response to immunotherapy with check-

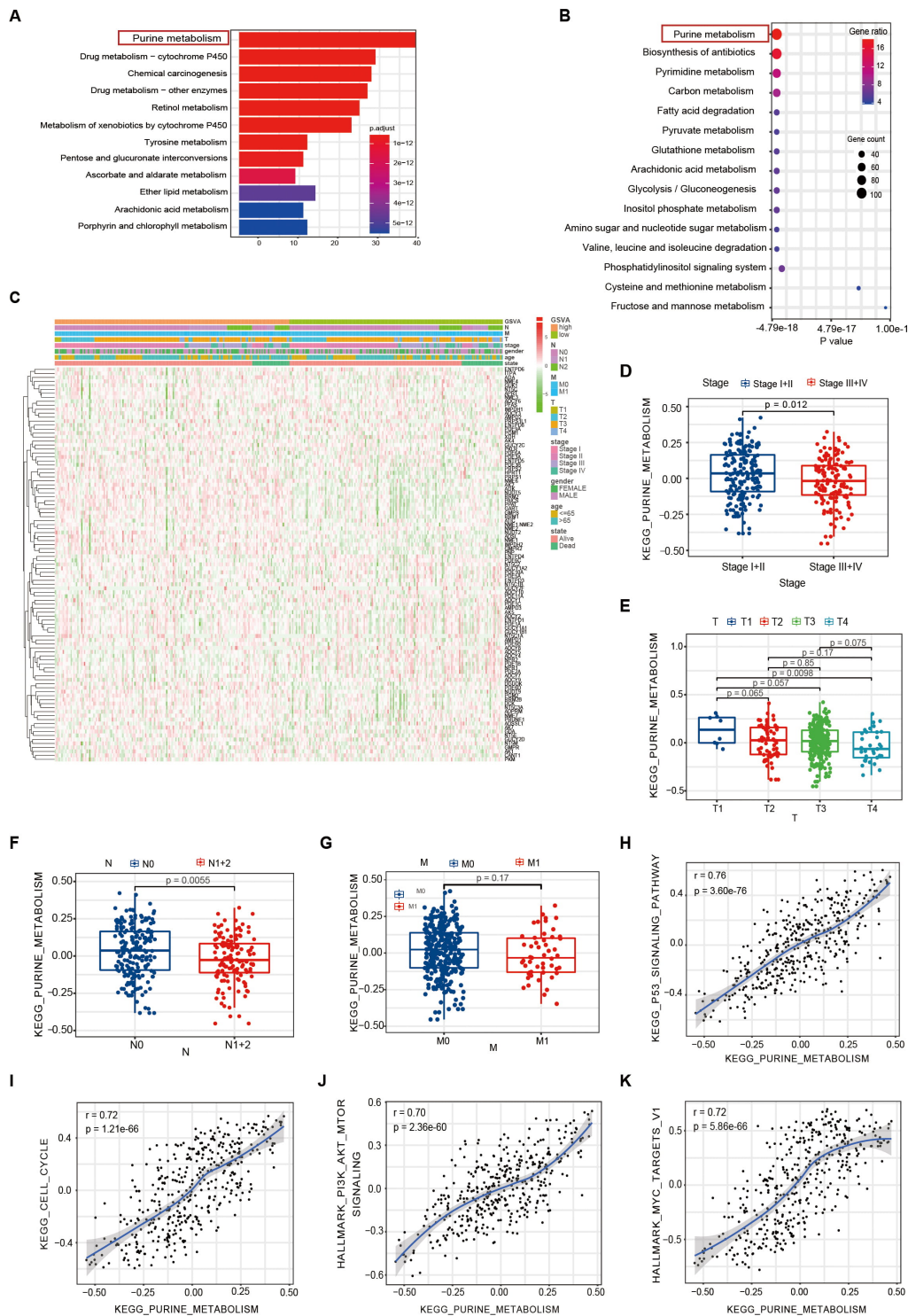


Fig. 3. Purine metabolism is the most significantly altered pathway related to the prognosis of COAD, and plays an important role in the development of COAD. (A) The top 12 enriched pathways identified from KEGG analysis of the MRDEGs. The bar color changes gradually from blue to red in ascending order according to the adjusted p -values. (B) The top 15 enriched pathways identified from KEGG analysis of the MRPGs. The bar color changes gradually from blue to red in ascending order according to the adjusted p -values. The size of the node represents the number of counts. (C) Heatmap for the expression of purine metabolism genes. (D–G) Distribution of GSVA enrichment scores for purine metabolism stratified according to TNM stage. (H–K) Associations between purine metabolism and the P53, PI3K/AKT/mTOR, cell-cycle, and MYC signaling pathways, as assessed by GSVA enrichment scores. These pathways were activated together with purine metabolism. KEGG, The Kyoto Encyclopedia of Genes and Genomes; GSVA, Gene Set Variation Analysis; TNM, tumor-node-metastasis.

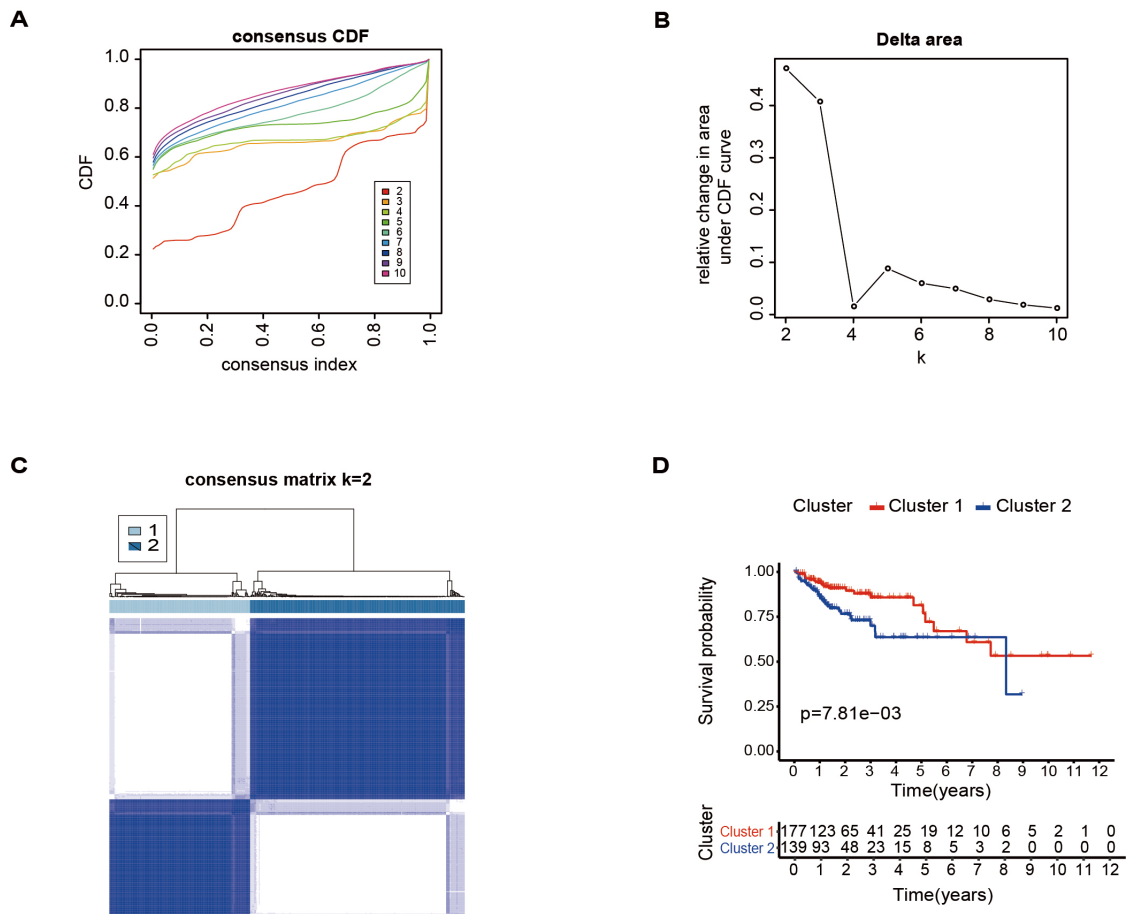


Fig. 4. The expression of purine metabolism genes is closely related to the survival of COAD patients. (A) Consensus clustering cumulative distribution function for $k = 2$ to $k = 10$. (B) Relative change in the area under the CDF curve for $k = 2$ to $k = 10$. (C) Consensus clustering matrix for $k = 2$. (D) K-M survival curves for patients in the two clusters.

point inhibitors. The expression of immune checkpoints was therefore investigated in the two subtypes. Patients in cluster-2 expressed higher levels of *PDI*, *PD-L1*, *PD-L2*, *LGALS9*, *HAVCR2*, *CD86*, *CD80*, *CTLA4*, *TNFRSF9* and *TNFSF9* than patients in cluster-1 (Fig. 5B–K), indicating they may respond better to immunotherapy.

The distribution of 22 immune cell types in the two subgroups was compared using the CIBERSORT algorithm. Cluster-1 showed higher levels of infiltration with monocytes and CD4 memory-resting T cells, whereas cluster-2 showed more CD8 T-cells, M1 macrophages, and follicular helper T cells (Fig. 5L).

3.6 Identification of Potential Immuno-Metabolic Checkpoints in COAD

Purine metabolism status had closely related to the expression of immune checkpoints [16,17]. Therefore, targeting of the purine metabolism pathway may be a potential strategy for improving the efficacy of immune blockade therapy. Pearson correlation analysis was used to compare the expression of genes in the purine metabolism pathway with immune checkpoints. With a cut-off point of $|R|$

>0.5 , we found 8 genes that were highly correlated with the expression of immune checkpoints. The expression of four of these genes (*GUCY1A1*, *GUCY1B1*, *PDE1A* and *PDE5A*) were significantly lower in COAD than normal tissues (Fig. 6A–D). Moreover, a similar expression pattern for these genes was seen in an independent patient cohort (GSE74602) (Supplementary Fig. 2A). IHC staining also revealed the expression of *GUCY1A1*, *GUCY1B1*, *PDE1A* and *PDE5A* were downregulated in COAD tissues (Fig. 6E, Supplementary Fig. 2B). As shown in Fig. 6F–K, *PD-L2* expression was positively correlated with the expression of *GUCY1A1* ($r = 0.55$, $p = 8.52 \times 10^{-34}$), *GUCY1B1* ($r = 0.55$, $p = 2.41 \times 10^{-33}$) and *PDE1A* ($r = 0.52$, $p = 6.05 \times 10^{-30}$). The expression of *CD80* was positively correlated to that of *GUCY1A1* ($r = 0.55$, $p = 1.44 \times 10^{-33}$) and *PDE5A* ($r = 0.56$, $p = 3.63 \times 10^{-35}$), while the expression of *CD86* was positively correlated with *GUCY1B1* expression ($r = 0.51$, $p = 5.24 \times 10^{-28}$). These findings suggest that targeting of *GUCY1A1*, *GUCY1B1*, *PDE1A* and *PDE5A* may improve the effectiveness of immunotherapy, especially in patients with higher *PDE1A* (Supplementary Fig. 2C).

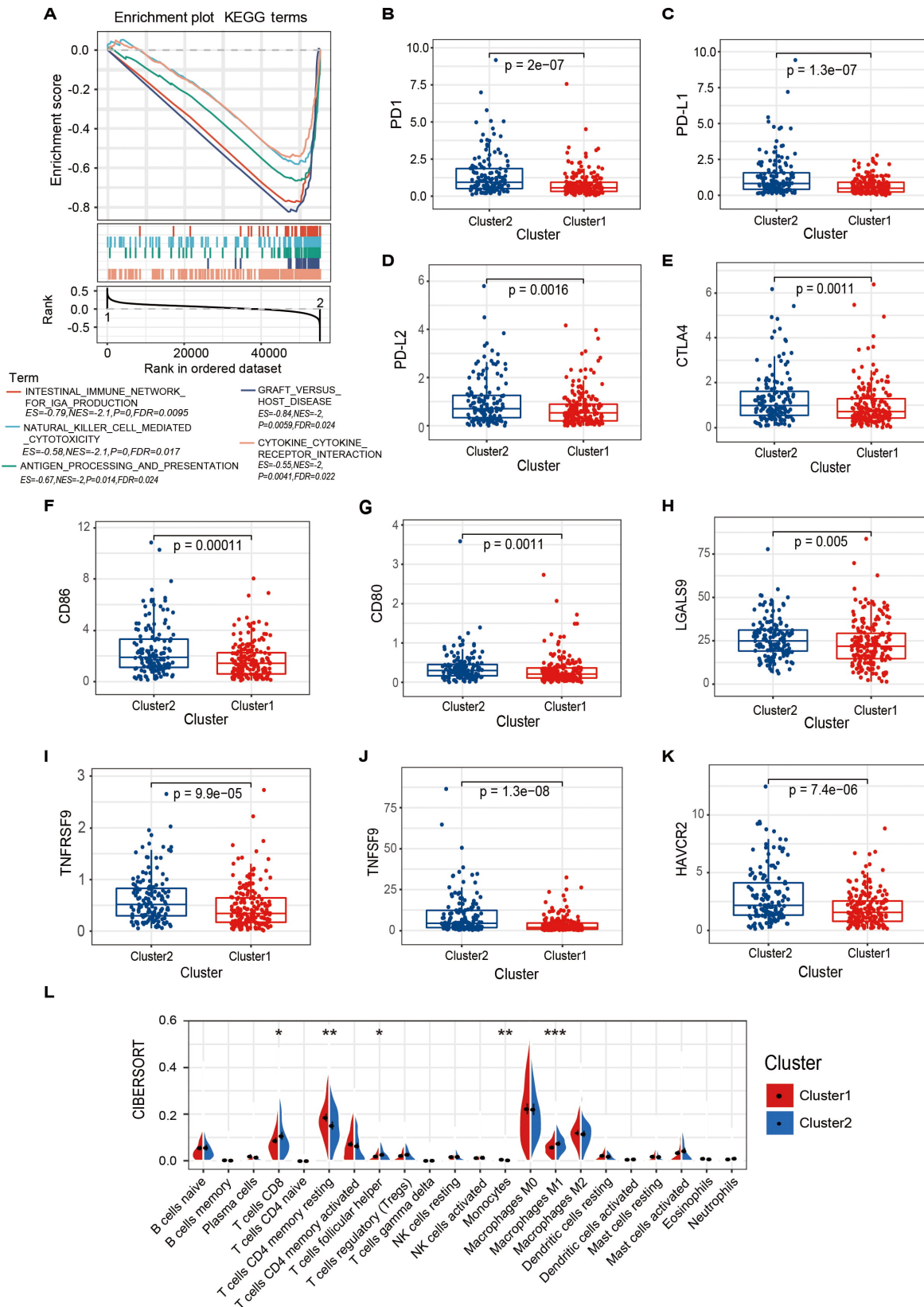


Fig. 5. Consensus clustering of purine metabolism genes with anti-tumor immunity. (A) GSEA showed that samples in cluster-2 were more likely to be enriched in immune-related pathways. (B–K) Expression levels for *PD1*, *PD-L1*, *PD-L2*, *LGALS9*, *HAVCR2*, *CD86*, *CD80*, *CTLA4*, *TNFRSF9* and *TNFSF9* in cluster-1 and cluster-2 subtypes from the TCGA cohort. (L) Infiltrating levels of 22 immune cell types in cluster-1 and cluster-2 subtypes from the TCGA cohort. * $p < 0.05$, ** $p < 0.01$ and *** $p < 0.001$. GSEA, Gene Set Enrichment Analysis.

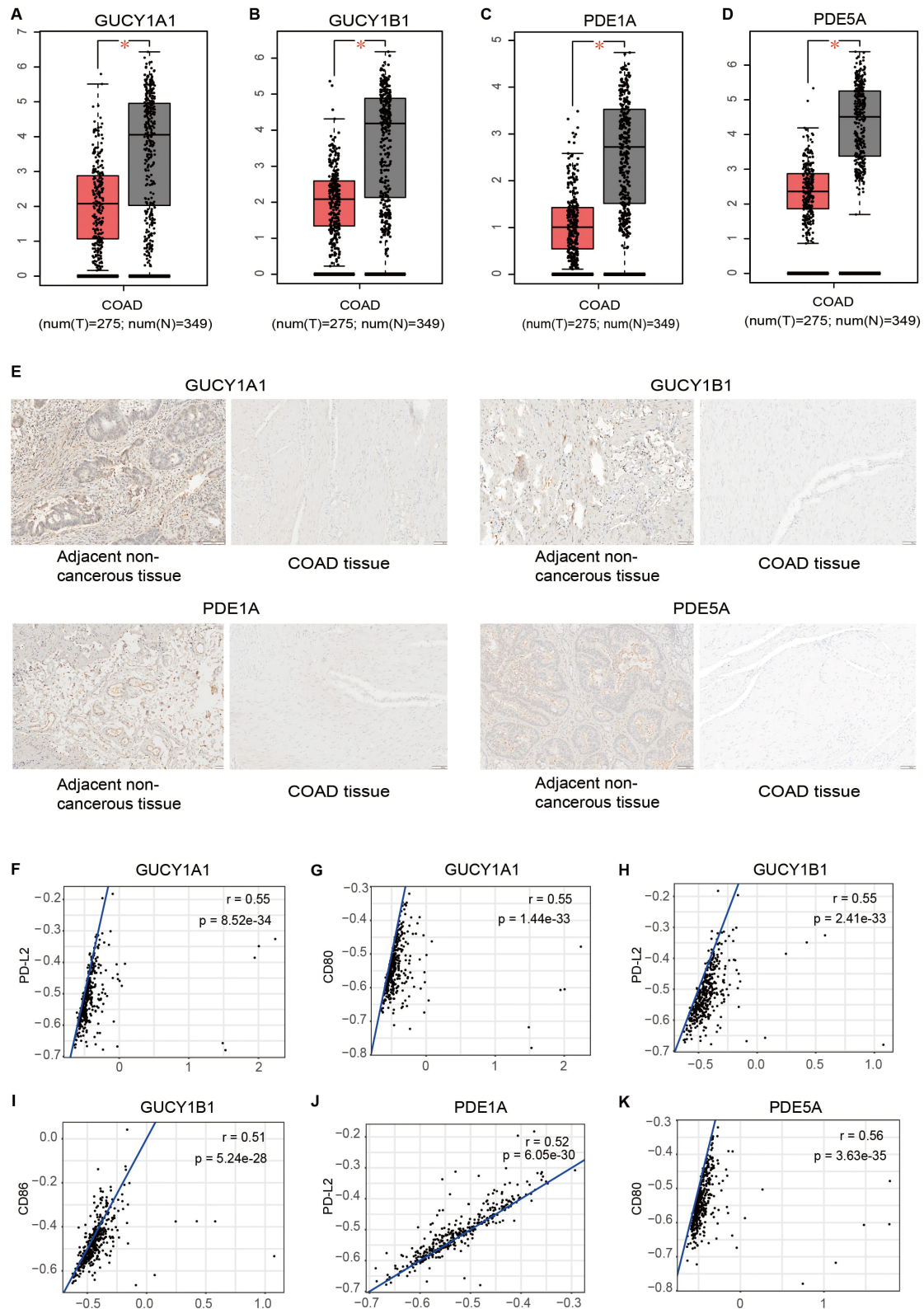


Fig. 6. Identification of potential immuno-metabolic checkpoints in COAD. (A–D) Expression levels for *GUCY1A1*, *GUCY1B1*, *PDE1A* and *PDE5A* in tumor and normal tissues from the GEPIA database. (E) IHC staining of *GUCY1A1*, *GUCY1B1*, *PDE1A* and *PDE5A* was significantly lower in COAD tissues compared to normal tissue. Scale bars represent 100 μm . (F,G) Correlation between the expression of immune checkpoints and *GUCY1A1* in the TCGA database. (H,I) Correlation between the expression of immune checkpoints and *GUCY1B1* in the TCGA database. (J) Correlation between the expression of *PD-L2* and *PDE1A* in the TCGA database. (K) Correlation between the expression of *CD80* and *PDE5A* in the TCGA database.

The heatmap shown in **Supplementary Fig. 2D** provides an overview of the correlation coefficients between the signature genes and the immune checkpoints. We found no significant difference in the expression of PDE6C, NT5C1B, ENTPD1 and AMPD3 between COAD and normal tissues (**Supplementary Fig. 3A–G**). However, the expression levels of PDE6C, NT5C1B, ENTPD1 and AMPD3 were also positively correlated to the expression of immune checkpoints (**Supplementary Fig. 3H–M**).

4. Discussion

Ever since the “Warburg effect” was first described, much attention has been paid to metabolic reprogramming. This concept has been pivotal in our understanding of tumor metabolism. In the present study, KEGG analysis of MRDEGs and MRPGs revealed the involvement of purine metabolism in COAD. Activation of the purine metabolism pathway plays a critical role in the development of COAD, TME function, and the efficacy of immunotherapy. Targeting of GUCY1A1, GUCY1B1, PDE1A or PDE5A in the purine metabolism pathway may improve the effectiveness of immune checkpoint blockade therapy.

Screening for MRDEGs identified *EPHX2*, *GPX3*, *PTGDS*, *NAT2*, *ACOX1*, and *CPT2* to have the strongest prognostic values. The expression and prognostic value of these genes in COAD were validated in independent datasets. In addition, we developed a risk score formula based on this 6-gene signature and validated its prognostic value. MRPGs were the genes that were highly correlated with the 6-gene signature ($|r| > 0.3$). KEGG analysis was performed separately for MRDEGs and MRPGs. Interestingly, the purine metabolism pathway was enriched not only with the strongest MRDEGs, but also with the MRPGs. These novel findings highlight the importance of purine metabolism in COAD. Impaired purine metabolism is known to be the major factor in gout pathogenesis. Purine nucleotides are also fundamental for tumor cell proliferation, and the major role of purine metabolism in tumors is well known [18,19]. Purine metabolism includes three main pathways: the *de novo* purine biosynthetic pathway, the purine salvage pathway, and the degradation pathway. A previous metabolomic study revealed how the purine metabolism pathway was reprogrammed [20]. Colorectal tumor tissues have higher levels of inositol monophosphate, adenosine, adenosine monophosphate, hypoxanthine and xanthine than normal tissues, as well as a lower level of uric acid. This indicates switching from the purine biosynthetic pathway to the more efficient salvage pathway during tumorigenesis [20]. The current transcriptome-level study highlights the importance of reprogrammed purine metabolism in the initiation and prognosis of COAD. Our novel findings extend the results of previous studies in this field.

Different stages of COAD tumors were shown here to have different purine metabolism enrichment scores. Moreover, GSVA enrichment scores for the purine metabolism pathway were strongly associated with pathways that promote COAD tumorigenesis ($|Cor| > 0.7$), thus demonstrating the involvement of purine metabolism in COAD. A previous study showed that metabolic reprogramming of colorectal cancer is mainly caused by aberrant *MYC* expression [21]. This could explain the strong correlation observed in the present study between reprogrammed purine metabolism and the *MYC* target signature. Target genes associated with PDE1A, PI3K/AKT/mTOR signaling, p53 signaling, and cell cycle pathway may lie downstream of the purine metabolism pathway [22–24].

Two tumor clusters were obtained by consensus clustering based on the expression of purine metabolism genes. The main clinical differences between these clusters were OS and anti-tumor immunity. We conclude that purine metabolism can reprogram the TME immune status, thereby impacting anti-tumor immunity and tumor prognosis. The purine nucleoside adenosine (ADO) is a product of purine metabolism and has an immunosuppressive effect [25]. ADO is able to suppress differentiation of monocytes into macrophages via the activation of A2 receptor signaling [25–27]. This could explain the different level of infiltration of monocytes and of M1 macrophages between the two clusters. Inosine is known to serve as an alternative carbon source for CD8⁺ T cells in the absence of glucose. It also enhances their tumor-killing ability and promotes the expression of effector molecules such as tumor necrosis factor alpha [28]. The current finding that purine metabolism has an important role in anti-tumor immunity is consistent with these earlier results.

Immune checkpoint blockade therapy has revolutionized cancer treatment due to its durable responses and fewer side-effects compared with conventional cancer treatments [29–31]. However, a considerable proportion of patients remain unresponsive to these treatments, while about one-third of patients relapse after the initial response and develop adaptive resistance [32]. In the present study, higher expression of immune checkpoints was observed in cluster-2 COAD patients, suggesting these patients may have better immunotherapy response. Therefore, the purine metabolism status of tumor may predict their response to immunotherapy. Current and future research strategies may involve targeting of the purine metabolism pathway, and the development of combination strategies to increase the efficacy of immunotherapy. The adenosinergic pathway forms a part of the purine metabolism pathway and represents an attractive target for cancer therapy. The ectonucleotidases CD39 and CD73, also known as ENTPD1 and NT5E, respectively, are critical mediators of adenosine accumulation in the TME [32,33]. Extensive pre-clinical experiments with colon cancer cells have shown promising results by targeting the adenosinergic pathway, including

CD39, CD73 and receptors for adenosine, in combination with chemotherapy or immunotherapy [34–37]. In the current study we identified 8 genes as potential targets for increasing the efficacy of immunotherapy. The expression of these genes was highly correlated with the expression of immune checkpoints. GUCY1A1 and GUCY1B1 are subunits of soluble guanylyl cyclase (sGC) and produce the second messenger cyclic GMP (cGMP). The role of sGC in other cancers has been reported [38,39], but there are currently no reports on its effectiveness for improving immunotherapy. We found that GUCY1A1 and GUCY1B1 were downregulated in COAD, and their expression was highly correlated with PD-L2, CD80 and CD86. PDE1A and PDE5A are members of the phosphodiesterase (PDE) family, which catalyze the hydrolysis of 3' cyclic phosphate bonds in adenosine and/or guanine 3',5' cyclic monophosphate [40]. PDE inhibitors have been used as a novel approach to treat colon cancer [41]. The present study is the first to show a strong correlation between the expression of PDEs (PDE1A and PDE5A) and immune checkpoints. Our study also found a strong correlation between the expression of CD39 (ENTPD1) and immune checkpoints (**Supplementary Fig. 3J–L**), consistent with the results of a previous study [34].

There are several limitations to our study. First, the relationship between reprogrammed purine metabolism and COAD prognosis was detected at the transcriptome level instead of protein level. Second, it is not known whether other metabolites in the purine metabolism pathway in addition to adenosine contribute to human tumor progression. Finally, only correlations between the expression of immune checkpoints and potential immuno-metabolic genes were identified, and further inference regarding causality cannot be drawn. Additional experiments are therefore required to justify this hypothesis.

5. Conclusions

This study highlights the importance of purine metabolism in the development of COAD, and identified several important metabolism-related genes involved in anti-tumor immunity. In particular, we identified four potential targets in purine metabolism that may increase the efficacy of immunotherapy. Our findings provide new insights into purine metabolism in cancer and serve as a vital reference for the discovery of new immune-metabolic checkpoints in COAD patient.

Availability of Data and Materials

The data that support the findings of this study are openly available in TCGA, GEO and ICGC. Data sources and handling of these data are described in the Materials and Methods section. Further details are available from the corresponding author upon request.

Author Contributions

TL, TZ contributed to conception and design of the study. TL, HL, YZ drafted the manuscript. TL, HL, YZ organized the database and performed the statistical analysis. TL, HL, QZ performed experiments and revised the manuscript. All authors commented on the manuscript. All authors read and approved the final manuscript. All authors have participated sufficiently in the work and agreed to be accountable for all aspects of the work.

Ethics Approval and Consent to Participate

The data from TCGA and GEO are both publicly available, the patients involved in the database have obtained ethical approval. Thus, the present study was exempted from the approval of local ethics committees. The current research follows the TCGA and GEO data access policies and publication guidelines. This study was approved by the Institutional Ethics Review Board of the Third People's Hospital of Chengdu (2021-S-90) and conducted following the Chinese ethical guidelines for human genome/gene research.

Acknowledgment

We thank many researchers that deposited their valuable public data sets in TCGA, GEO and ICGC.

Funding

This study was supported by Natural Science Foundation of Sichuan Province (2023NSFSC1886), Natural Science Foundation of Sichuan Province (2023NSFSC0739).

Conflict of Interest

The authors declare no conflict of interest.

Supplementary Material

Supplementary material associated with this article can be found, in the online version, at <https://doi.org/10.31083/j.fbl2812328>.

References

- [1] Bray F, Ferlay J, Soerjomataram I, Siegel RL, Torre LA, Jemal A. Global cancer statistics 2018: GLOBOCAN estimates of incidence and mortality worldwide for 36 cancers in 185 countries. *CA: A Cancer Journal for Clinicians*. 2018; 68: 394–424.
- [2] Hanahan D, Weinberg RA. Hallmarks of cancer: the next generation. *Cell*. 2011; 144: 646–674.
- [3] Yoshida GJ. Metabolic reprogramming: the emerging concept and associated therapeutic strategies. *Journal of Experimental & Clinical Cancer Research: CR*. 2015; 34: 111.
- [4] WEINHOUSE S. On respiratory impairment in cancer cells. *Science (New York, N.Y.)*. 1956; 124: 267–269.
- [5] Carracedo A, Cantley LC, Pandolfi PP. Cancer metabolism: fatty acid oxidation in the limelight. *Nature Reviews. Cancer*. 2013; 13: 227–232.
- [6] Michalek RD, Gerriets VA, Jacobs SR, Macintyre AN, MacIver NJ, Mason EF, *et al*. Cutting edge: distinct glycolytic and lipid oxidative metabolic programs are essential for effector and regulatory CD4+ T cell subsets. *Journal of Immunology (Baltimore, Md.: 1950)*. 2011; 186: 3299–3303.

- [7] Ngwa VM, Edwards DN, Philip M, Chen J. Microenvironmental Metabolism Regulates Antitumor Immunity. *Cancer Research*. 2019; 79: 4003–4008.
- [8] Pavlova NN, Thompson CB. The Emerging Hallmarks of Cancer Metabolism. *Cell Metabolism*. 2016; 23: 27–47.
- [9] Brand A, Singer K, Koehl GE, Kolitzus M, Schoenhammer G, Thiel A, *et al.* LDHA-Associated Lactic Acid Production Blunts Tumor Immunosurveillance by T and NK Cells. *Cell Metabolism*. 2016; 24: 657–671.
- [10] Chen S, Cao G, Wu W, Lu Y, He X, Yang L, *et al.* Mining novel cell glycolysis related gene markers that can predict the survival of colon adenocarcinoma patients. *Bioscience Reports*. 2020; 40: BSR20201427.
- [11] Gill KS, Fernandes P, O'Donovan TR, McKenna SL, Doddakula KK, Power DG, *et al.* Glycolysis inhibition as a cancer treatment and its role in an anti-tumour immune response. *Biochimica et Biophysica Acta*. 2016; 1866: 87–105.
- [12] Goossens P, Rodriguez-Vita J, Etzerodt A, Masse M, Rastoin O, Gouirand V, *et al.* Membrane Cholesterol Efflux Drives Tumor-Associated Macrophage Reprogramming and Tumor Progression. *Cell Metabolism*. 2019; 29: 1376–1389.e4.
- [13] Ramapriyan R, Caetano MS, Barsoumian HB, Mafra ACP, Zambalde EP, Menon H, *et al.* Altered cancer metabolism in mechanisms of immunotherapy resistance. *Pharmacology & Therapeutics*. 2019; 195: 162–171.
- [14] Hänzelmann S, Castelo R, Guinney J. GSVA: gene set variation analysis for microarray and RNA-seq data. *BMC Bioinformatics*. 2013; 14: 7.
- [15] Uhlén M, Fagerberg L, Hallström BM, Lindskog C, Oksvold P, Mardinoglu A, *et al.* Proteomics. Tissue-based map of the human proteome. *Science (New York, N.Y.)*. 2015; 347: 1260419.
- [16] Saveljeva S, Sewell GW, Ramshorn K, Cader MZ, West JA, Clare S, *et al.* A purine metabolic checkpoint that prevents autoimmunity and autoinflammation. *Cell Metabolism*. 2022; 34: 106–124.e10.
- [17] Mager LF, Burkhard R, Pett N, Cooke NCA, Brown K, Ramay H, *et al.* Microbiome-derived inosine modulates response to checkpoint inhibitor immunotherapy. *Science (New York, N.Y.)*. 2020; 369: 1481–1489.
- [18] Ludwig N, Gillespie DG, Reichert TE, Jackson EK, Whiteside TL. Purine Metabolites in Tumor-Derived Exosomes May Facilitate Immune Escape of Head and Neck Squamous Cell Carcinoma. *Cancers*. 2020; 12: 1602.
- [19] Yin J, Ren W, Huang X, Deng J, Li T, Yin Y. Potential Mechanisms Connecting Purine Metabolism and Cancer Therapy. *Frontiers in Immunology*. 2018; 9: 1697.
- [20] Ong ES, Zou L, Li S, Cheah PY, Eu KW, Ong CN. Metabolic profiling in colorectal cancer reveals signature metabolic shifts during tumorigenesis. *Molecular & Cellular Proteomics: MCP*. 2010. (online ahead of print)
- [21] Satoh K, Yachida S, Sugimoto M, Oshima M, Nakagawa T, Akamoto S, *et al.* Global metabolic reprogramming of colorectal cancer occurs at adenoma stage and is induced by MYC. *Proceedings of the National Academy of Sciences of the United States of America*. 2017; 114: E7697–E7706.
- [22] Duan S, Huang W, Liu X, Liu X, Chen N, Xu Q, *et al.* IMPDH2 promotes colorectal cancer progression through activation of the PI3K/AKT/mTOR and PI3K/AKT/FOXO1 signaling pathways. *Journal of Experimental & Clinical Cancer Research: CR*. 2018; 37: 304.
- [23] Fang M, Shen Z, Huang S, Zhao L, Chen S, Mak TW, *et al.* The ER UDPase ENTPD5 promotes protein N-glycosylation, the Warburg effect, and proliferation in the PTEN pathway. *Cell*. 2010; 143: 711–724.
- [24] Vogelstein B, Lane D, Levine AJ. Surfing the p53 network. *Nature*. 2000; 408: 307–310.
- [25] Kumar V. Adenosine as an endogenous immunoregulator in cancer pathogenesis: where to go? *Purinergic Signalling*. 2013; 9: 145–165.
- [26] Arnaud-Sampaio VF, Rabelo ILA, Bento CA, Glaser T, Bezerra J, Coutinho-Silva R, *et al.* Using Cytometry for Investigation of Purinergic Signaling in Tumor-Associated Macrophages. *Cytometry. Part a: the Journal of the International Society for Analytical Cytology*. 2020; 97: 1109–1126.
- [27] Najjar HM, Ruhl S, Bru-Capdeville AC, Peters JH. Adenosine and its derivatives control human monocyte differentiation into highly accessory cells versus macrophages. *Journal of Leukocyte Biology*. 1990; 47: 429–439.
- [28] Wang T, Gnanaprakasam JNR, Chen X, Kang S, Xu X, Sun H, *et al.* Inosine is an alternative carbon source for CD8⁺-T-cell function under glucose restriction. *Nature Metabolism*. 2020; 2: 635–647.
- [29] Mahoney KM, Rennert PD, Freeman GJ. Combination cancer immunotherapy and new immunomodulatory targets. *Nature Reviews. Drug Discovery*. 2015; 14: 561–584.
- [30] Topalian SL, Drake CG, Pardoll DM. Immune checkpoint blockade: a common denominator approach to cancer therapy. *Cancer Cell*. 2015; 27: 450–461.
- [31] Wu D, Wang X, Xue Y, Sun C, Zhang M. Identification of a novel immune-related lncRNA signature to predict prognostic outcome and therapeutic efficacy of LGG. *Journal of Integrative Neuroscience*. 2022; 21: 55.
- [32] Vijayan D, Young A, Teng MWL, Smyth MJ. Targeting immunosuppressive adenosine in cancer. *Nature Reviews. Cancer*. 2017; 17: 765.
- [33] Zimmermann H, Zebisch M, Sträter N. Cellular function and molecular structure of ecto-nucleotidases. *Purinergic Signalling*. 2012; 8: 437–502.
- [34] Allard B, Pommey S, Smyth MJ, Stagg J. Targeting CD73 enhances the antitumor activity of anti-PD-1 and anti-CTLA-4 mAbs. *Clinical Cancer Research: an Official Journal of the American Association for Cancer Research*. 2013; 19: 5626–5635.
- [35] Beavis PA, Milenkovski N, Henderson MA, John LB, Allard B, Loi S, *et al.* Adenosine Receptor 2A Blockade Increases the Efficacy of Anti-PD-1 through Enhanced Antitumor T-cell Responses. *Cancer Immunology Research*. 2015; 3: 506–517.
- [36] Leone RD, Sun IM, Oh MH, Sun IH, Wen J, Englert J, *et al.* Inhibition of the adenosine A2a receptor modulates expression of T cell coinhibitory receptors and improves effector function for enhanced checkpoint blockade and ACT in murine cancer models. *Cancer Immunology, Immunotherapy: CII*. 2018; 67: 1271–1284.
- [37] Michaud M, Martins I, Sukkurwala AQ, Adjemian S, Ma Y, Pellegatti P, *et al.* Autophagy-dependent anticancer immune responses induced by chemotherapeutic agents in mice. *Science (New York, N.Y.)*. 2011; 334: 1573–1577.
- [38] Mohammadoo Khorasani M, Karami Tehrani F, Parizadeh SMR, Atri M. Differential expression of alternative transcripts of soluble guanylyl cyclase, GYCY1a3 and GUCY1b3 genes, in the malignant and benign breast tumors. *Nitric Oxide: Biology and Chemistry*. 2019; 83: 65–71.
- [39] Tuttle TR, Takiar V, Kumar B, Kumar P, Ben-Jonathan N. Soluble guanylate cyclase stimulators increase sensitivity to cisplatin in head and neck squamous cell carcinoma cells. *Cancer Letters*. 2017; 389: 33–40.
- [40] SUTHERLAND EW, RALL TW. Fractionation and characterization of a cyclic adenosine nucleotide formed by tissue particles. *The Journal of Biological Chemistry*. 1958; 232: 1077–1091.
- [41] Mehta A, Patel BM. Therapeutic opportunities in colon cancer: Focus on phosphodiesterase inhibitors. *Life Sciences*. 2019; 230: 150–161.